7536 *Inorg. Chem.* **2010**, *49*, 7536–7544
DOI: 10.1021/ic1009384

Inorganic Chemistry
Article

Structural Characterization of Zinc and Iron (II/III) Complexes of a Porphyrin Bearing Two Built-in Nitrogen Bases. An Example of High-Spin Diaqua-Iron(III) Bromo Complex

Ismail Hijazi, Thierry Roisnel, Pascale Even-Hernandez, Florence Geneste, Olivier Cador, Thierry Guizouarn, and Bernard Boitrel*

Université de Rennes1, Sciences Chimiques de Rennes, UMR CNRS 6226, 35042 Rennes Cedex, France

Received May 11, 2010

A bis-strapped porphyrin with two intramolecular nitrogen bases was synthesized, and its zinc(II), iron(II), and iron(III) complexes have been structurally characterized. Whereas the zinc(II) complex is square pyramidal five-coordinate and the iron(II) complex is six-coordinate despite a significant distortion of the macrocycle induced by the rigidity of the straps, the iron(III) complex exhibits a peculiar bis-aqua structure in which no intramolecular axial base is bound to the iron atom in the porphyrin. Furthermore, on one side, the bromide counteranion of the iron is bound inside the cycle formed by a strap and establishes a hydrogen bond with an axially bound water molecule. On the other side, a residual HBr molecule protonates one pyridine base leading to the formation of an intermolecular pyridinium−pyridine hydrogen bond. The large ionic radius of the high-spin iron(III) cation is accommodated in the macrocycle with no displacement of the metal out of the mean porphyrinic plane, with an average Fe−Np bond distance of 2.057 Å, and the axial Fe-Ow(aqua) bond distance measured at 2.090 Å. As a result, this high-spin iron(III) bis-aqua complex is only lightly distorted.

Introduction

The structural and electronic effects of peripheral substitution of the porphyrin macrocycle have been studied significantly in terms of reactivity, porphyrin distortion, and spin state.[1] Besides this type of derivatization at the periphery of the macrocycle, the coordination environment can also directly influence the planarity and the properties of the heme, as for instance in cytochrome c oxidase[2] (CcO) or dioxygen carriers.[3] Indeed, such tetrapyrrole distortions are believed to modulate biological functions of these hemoproteins, and obviously, the study of these distortions is greatly aided by X-ray structural data. This situation is particularly true in the domain of biomimetic heme analogues, in which chemists attempt to reproduce enzyme function with simple but sophisticated synthetic models.[4] Various structural features, such as the presence and number of axial ligand(s), the selective functionalization of the proximal or distal side of the heme, and the nature of other groups at the periphery of the distal pocket, are appropriate examples of this "functional tuning". For instance, our group has recently reported a general synthesis for CcO modeling (Scheme 1).[5] By this synthesis, together with model compounds **1** and **4** similarly functionalized on each side of the macrocycle, it is possible to prepare in one step a model, such as **5**, which possesses on one side a secondary coordination site for copper and on the other side a potential axial ligand for iron in the porphyrin. However, from the point of view of coordination chemistry, the precise behavior of such models is not always easy to envisage in as much as the structure and rigidity of the ligand itself as well as the synthetic procedure leading to the complex can influence significantly the coordination sphere of the metal. Of particular importance are porphyrin models bearing one or two intramolecular

*Corresponding author. Telephone: +33(2)2323 5856. Fax: +33(2)2323 5637. E-mail: Bernard.Boitrel@univ-rennes1.fr.

(1) (a) Barkigia, K. M.; Palacio, M.; Sun, Y.; Nogues, M.; Renner, M. W.; Varret, F.; Battioni, P.; Mansuy, D.; Fajer, J. *Inorg. Chem.* **2002**, *41*, 5647–5649. (b) Kadish, K. M.; Lin, M.; Van Caemelbecke, E.; De Stefano, G.; Medforth, C. J.; Nurco, D. J.; Nelson, N. Y.; Krattinger, B.; Muzzi, C. M.; Jaquinod, L.; Xu, Y.; Shyr, D. C.; Smith, K. M.; Shelnutt, J. A. *Inorg. Chem.* **2002**, *41*, 6673–6687. (c) Song, Y. J.; Haddad, R. E.; Jia, S. L.; Hok, S.; Olmstead, M. M.; Nurco, D. J.; Schore, N. E.; Zhang, J.; Ma, J. G.; Smith, K. M.; Gazeau, S.; Pecaut, J.; Marchon, J. C.; Medforth, C. J.; Shelnutt, J. A. *J. Am. Chem. Soc.* **2005**, *127*, 1179–1192. (d) Hu, C.; An, J.; Noll, B. C.; Schulz, C. E.; Scheidt, W. R. *Inorg. Chem.* **2006**, *45*, 4177–4185.

(2) Yoshikawa, S., Reducing Dioxygen to Water: Cytochrome c Oxidase. In *Biological Inorganic Chemistry. Structure and Reactivity*; Bertini, I., Gray, H. B., Stiefel, E. I., Valentine, J. S., Eds.; University Science Books: Sausalito, CA, 2000; pp 413−426.

(3) Jameson, G. B.; Ibers, J. A., Dioxygen Carriers. In *Biological Inorganic Chemistry. Structure and Reactivity*, ed.; Bertini, I.; Gray, H. B.; Stiefel, E. I.; Valentine, J. S.; University Science Books: Sausalito, 2000; pp 319−331.

(4) (a) Kim, E.; Chufan, E. E.; Kamaraj, K.; Karlin, K. D. *Chem. Rev.* **2004**, *104*, 1077–1133. (b) Collman, J. P.; Boulatov, R.; Sunderland, C. J.; Fu, L. *Chem. Rev.* **2004**, *104*, 561–588.

(5) Ruzié, C.; Even-Hernandez, P.; Boitrel, B. *Org. Lett.* **2008**, *10*, 2673–2676.

 Published on Web 07/13/2010

Scheme 1. General Synthetic Strategy Leading to Porphyrin **1** among Two Other Models **4** and **5**

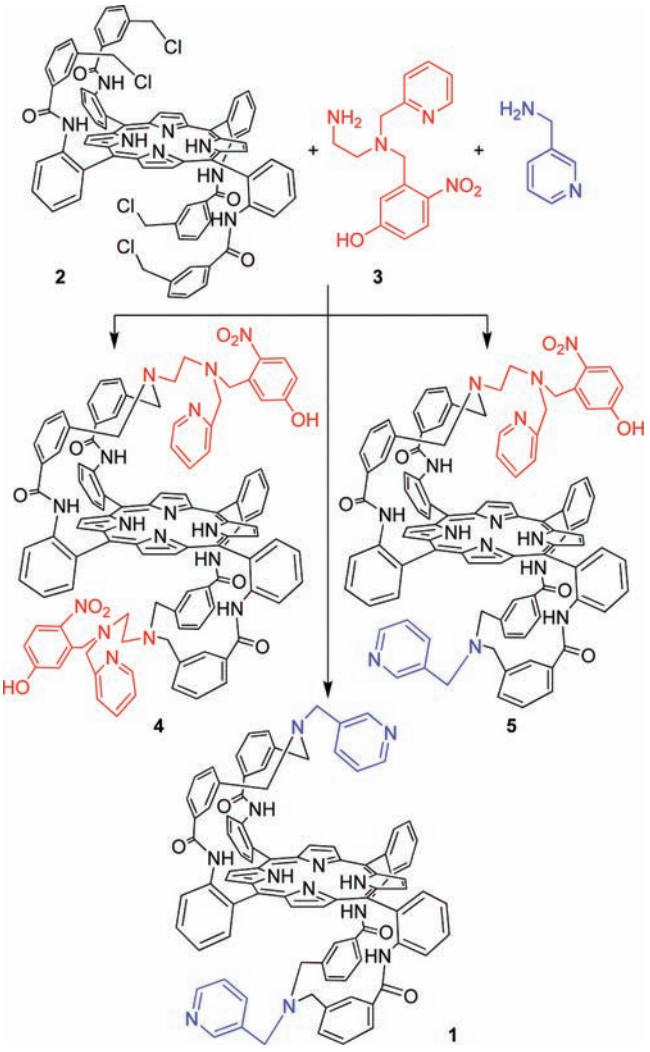

nitrogen bases as their behavior can differ significantly, as illustrated in several previous reports. For instance, basket-handle porphyrins bearing one or two pyridine groups incorporated in the strap were synthesized, either with ether[6] or amide linkages.[7] However, in both cases, incorporation of iron(II) led to either the five- or the six-coordinate complex for the model bearing one or two pyridines, respectively. The influence of the nitrogen base has also been investigated toward the affinity of dioxygen adducts with so-called twin-coronet iron(II) porphyrins.[8] The dioxygen affinity of the complex bearing a tailed imidazole was greater by an order of magnitude than that with a tailed pyridine. Interestingly, the X-ray structure of a model of CcO in which a 2-pyridyl arm of the copper chelate migrated to the iron center leading to a five-coordinate complex was recently reported.[9] Despite the steric hindrance due to the linkage in ortho position of the pyridine cycle, the latter was able to bind the iron but with an angle to the 24-atom mean plane close to 85°. Similarly, we report herein structural data of metalated porphyrins bearing two axial pyridine residues. We display how a specific ligand leads not only to the expected five-coordinate zinc complex and six-coordinate highly distorted iron(II) complex but also to an unexpected and scarce bis-aqua iron(III) lightly distorted complex, despite the presence of two intramolecular nitrogen bases.

(6) Momenteau, M.; Mispelter, J.; Loock, B.; Lhoste, J.-M. *J. Chem. Soc., Perkin Trans. I* **1985**, 61–70.
(7) Momenteau, M.; Mispelter, J.; Loock, B.; Lhoste, J.-M. *J. Chem. Soc., Perkin Trans. I* **1985**, 221–231.
(8) Tani, F.; Matsu-ura, M.; Ariyama, K.; Setoyama, T.; Shimada, T.; Kobayashi, S.; Hayashi, T.; Matsuo, T.; Hisaeda, Y.; Naruta, Y. *Chem.—Eur. J.* **2003**, *9*, 862–870.
(9) Kim, E.; Helton, M. E.; Lu, S.; Moenne Loccoz, P.; Incarvito, C. D.; Rheingold, A. L.; Kaderli, S.; Zuberbuhler, A. D.; Karlin, K. D. *Inorg. Chem.* **2005**, *44*, 7014–7029.

Experimental Section

Materials and Methods. All commercial chemicals (Aldrich, Acros) and solvents (ACS for analysis) were used without further purification unless otherwise stated. Solvents used in an inert atmosphere (drybox; $[O_2]$: < 1 ppm) were freshly distilled and deoxygenated by three "freeze-pump" cycles. Benzene, toluene, and THF were distilled over potassium benzophenone ketyl; methylene chloride, pyridine, triethylamine and pentane over CaH_2; and methanol over magnesium turnings. Column chromatographies were performed on SiO_2 (Merck TLC-Kieselgel 60H, 15 μm). Mass spectra EI: Varian MAT 33 spectrometer and ESI: Micromass MS/MS ZABSpec TOFF spectrometer were performed at the C.R.M.P.O. (University of Rennes 1). ^{1}H and ^{13}C NMR spectra were recorded on Bruker Avance 500 or 300 spectrometers equipped with a TBI probe or a Bruker Avance 300 spectrometer with a BBO probe. Spectra were referenced with residual solvent protons. UV−vis spectra were recorded on an Uvikon XL spectrometer. X-ray data were collected on an APEXII, Bruker-AXS diffractometer. Voltammetric experiments were carried out using an EDAQ potentiostat unit, with the EChem software package. A vitreous carbon rotating disk electrode (Radiometer-Tacussel) as working electrode, a platinum wire auxiliary electrode, and a saturated calomel reference electrode (SCE) were used in a standard three-electrode configuration. Voltammetric analyses were performed in acetonitrile, containing 0.1 M tetrabutylammonium hexafluorophosphate under a dinitrogen atmosphere. Magnetization measurement was performed on a powdered sample with a Quantum Design MPMS-XL SQUID magnetometer operating in a 2−300 K temperature range with dc external magnetic up to 5 T. The data have been corrected from the sample holder contribution as well as from the core diamagnetism estimated from Pascal's tables. The electron paramagnetic resonance (EPR) spectrum was recorded on the same powdered sample used for magnetization dissolved in chloroform at liquid helium temperature (4.2 K) with a BRUKER EMX X-band spectrometer equipped with an Oxford cryostat.

Synthesis and Characterization. Porphyrin **1** has been synthesized as previously described.[5]

α-5,10-*β*-15,20-Bis(2,2′-{3,3′-[*N*,*N*-(Pyridin-3-ylmethyl)amine]-dibenzoylamino}diphenyl)zinc(II) Porphyrin, 1Zn. To a solution of porphyrin **1** (0.008 mmol, 8 mg) in a methanol/chloroform (1/5) mixture (5 mL) was added sodium acetate (0.1 mmol, 18 mg) and zinc acetate (0.1 mmol, 8 mg). The mixture was heated overnight at 60 °C, and then solvent was removed under vacuum. The resulting powder was dissolved in chloroform and washed with NaOH 2N, dried over $MgSO_4$, and concentrated in vacuum. The resulting powder was dissolved in chloroform and directly loaded on a silica gel chromatography. The expected compound eluted with $CHCl_3$ was obtained in 92% yield (8 mg). ^{1}H NMR (500.13 MHz, DMSO-d_6, 383 K): δ = 8.87 (s, 4H, $H_{\beta pyr}$); 8.64 (s, 4H, $H_{\beta pyr}$); 8.54 (broad s, 4H, −N*H*CO); 8.41 (d, 4H, J = 8.1 Hz, H_3); 7.79 (t, 4H, J = 7.8 Hz, H_4); 7.62 (d, 4H, J = 7.1 Hz, H_6); 7.43 (d, 4H, J = 8.1 Hz, $H_{6'}$); 7.39 (t, 4H, J = 7.3 Hz, H_5); 7.02 (t, 4H, J = 7.6 Hz, $H_{5'}$); 6.75 (app. t, 6H, ^3J = 8.1 Hz, $H_{4'} + H_{4pyr}$); 6.59 (dd, 2H, ^3J = 7.6 and ^3J = 4.9 Hz, H_{5pyr}); 6.10 (broad s, 2H, H_{2pyr}); 5.69 (broad s, 2H, H_{6pyr}); 4.88 (s, 4H, $H_{2'}$); 1.71 (s, 4H, H_b); 1.58 (d, 4H,

J = 12.6 Hz, H_a); 1.17 (d, 4H, J = 12.6 Hz, H_a). HR-MS (ESI-MS): calcd m/z = 1439.4363 for $C_{88}H_{64}N_{12}O_4Na^{64}Zn$ $[M + Na]^+$, found 1439.4357. UV−vis (CH_2Cl_2): λ/ nm ($10^{-3}\varepsilon$, dm^3 mol^{-1}cm^{-1}): 411.0 (35.2), 433.0 (329.6), 524.0 (3.3), 562.0 (14.6), 600.0 (3.4).

α-5,10-β-15,20-Bis(2,2′-{3,3′-[*N*,*N*-(Pyridin-3-ylmethyl)amine]-dibenzoylamino}diphenyl)iron(III) Porphyrin Bromide, 1Fe(III). In a drybox, to a solution of porphyrin **1** (0.014 mmol, 20 mg) in THF (6 mL) was added iron(II) bromide (0.1 mmol, 20 mg). The mixture was stirred overnight at 65 °C in a Schlenk tube. After removal of the solvent, the iron complex was taken out the drybox and purified in its oxidized state by preparative layer chromatography. The expected compound eluted with 1% MeOH/$CHCl_3$/$NH_{3\ g}$ was obtained in 94% yield (18.73 mg). HR-MS (LSIMS-MS): calcd m/z = 1408.45229 for $C_{88}H_{64}N_{12}O_4{}^{56}Fe$ $[M]^{+\bullet}$, found 1408.4553.

α-5,10-β-15,20-Bis(2,2′-{3,3′-[*N*,*N*-(Pyridin-3-ylmethyl)amine]-dibenzoylamino}diphenyl)iron(II) Porphyrin, 1Fe(II). In a drybox, compound **1Fe(III)** (0.007 mmol, 10 mg) was dissolved in toluene (7 mL), and a saturated aqueous solution of $Na_2S_2O_4$ was added. After 5 min of stirring, the organic layer was dried over $MgSO_4$ and evaporated. The product was precipitated and dried under vacuum (quantitative yield). ^{1}H NMR ($CDCl_3$, 300 K, Young NMR tube): δ = 9.03 (d, 4H, J = 8.1 Hz, H_3); 8.83 (s, 4H, $H_{\beta pyr}$); 8.66 (app. d, 8H, $H_{\beta pyr}$ + N*H*CO); 8.04 (d, 4H, J = 7.8 Hz, $H_{4'}$); 7.67 (t, 4H, J = 7.8 Hz, H_4); 7.26 (4H, $H_{5'}$); 7.13 (t, 4H, J = 7.3 Hz, H_5); 6.99 (d, 4H, J = 7.1 Hz, $H_{6'}$); 7.43 (d, 4H, J = 8.1 Hz, H_6); 5.87 (d, 2H, ^3J = 7.6 and ^3J = 4.9 Hz, H_{5pyr}); 5.16 (broad s, 2H, ^3J = 8.1 Hz, H_{4pyr}); 3.77 (app. s, 2H, H_{6pyr}); 2.82 (s, 4H, H_b); 2.36 (s, 4H, $H_{b'}$); 1.99 (s, 4H, $H_{2'}$); 1.87 (broad s, 2H, H_{2pyr}); 1.30 (app. m, 4H, H_a); 0.99 (app. t, 4H, J = 12.6 Hz, $H_{a'}$).

X-ray Crystallographic Studies. Crystallographic data (excluding structure factors) for the structures reported in this paper have been deposited with the Cambridge Crystallographic Data Center as supplementary publication nos. CCDC 771833 (**1Zn**), CCDC 771834 (**1Fe(II)**), and CCDC 771835 (**1Fe(III)**). Copies of the data can be obtained free of charge on application to the CCDC, 12 Union Road, Cambridge CB2 1EZ, U.K. (fax, (international) + 44−1223/336−033; e-mail, deposit@ccdc.ca-m.ac.uk). The structures were solved by direct methods using the SIR97 program,[10] which revealed all the non-hydrogen atoms, and refined with full-matrix least-squares methods based on $F2$ (SHELX-97)[11] with the aid of the WINGX19[12] program. All non-hydrogen atoms were refined with anisotropic thermal parameters. Hydrogen atoms were finally included in their calculated positions.

Results and Discussion

As previously mentioned, we have reported two different series of synthetic models of either cytochrome c oxidase (CcO)[5] or dioxygen carriers[13] which exhibit interesting properties owing to the design of their distal side. However, in both series, a critical prerequisite is the coordination of the intramolecular nitrogen base to the iron center to ensure a five coordination of the metal and thus, to obtain models in which a coordination site remains available for dioxygen binding. In the case of the CcO models, the synthetic pathway consisted of reacting two nucleophilic reagents with a four-electrophilic picket porphyrin leading to three porphyrins. One of them has two different sides and the two others, considered as side products, exhibit the same functionalization on each side. Among these two side products, porphyrin **1**, bears two intramolecular pyridine cycles (Scheme 2). Where the iron(II) complex of such a ligand is not expected to be very reactive for the binding of small molecules, for example, the particular structure of its iron(III) complex prompted us to investigate the coordination behavior of this porphyrin with various metals. Conversely to our previous report,[5] for the purposes of this work, this symmetrical porphyrin **1** was synthesized by a direct pathway that chiefly consists of reacting 4 equivalents of *C*-pyridin-3-yl-methylamine with α-5,10-β-15,20-tetrakis{2-[(3-chloromethyl) benzoylamino]phenyl} porphyrin.

In order to verify de facto the possible intramolecular coordination of the nitrogen base, we first inserted zinc inside porphyrin **1**, as it is known that the resulting complex should be five-coordinate although six-coordinate zinc porphyrins cannot be ruled out, at least in the solid state.[14] This reaction was performed by the usual method of heating at 60 °C the porphyrin in a mixture of $CHCl_3$/ MeOH with zinc acetate and sodium acetate. This results in a Soret red shift from 424 nm for the free-base to 433 nm for the zinc complex. In solution, proton NMR spectroscopy revealed an upfield shift of the protons of the pyridine cycles, particularly for the two protons H_2 and H_6 in ortho positions of the pyridine (Figure 1) relatively to the free base. Furthermore, whereas the signals of the pyridinic protons are sharp and well resolved in the free-base, they become broad in the zinc complex. This observation is consistent with a slow exchange of the axial ligands on the NMR time scale, and seems to indicate that, as expected, only one pyridine is coordinated to the zinc atom but exchanges slowly with the other one. Accordingly, an average position of the pyridine cycles, consistent with a moderated shielding of their protons, is observed by proton NMR spectroscopy.

A second obvious observation is relative to the AB system of the benzylic methylene groups of the straps. In the free-base compound, they resonate at 0.58 and 0.18 ppm as two well resolved doublets. In the zinc complex, they appear as broad singlets at 1.50 and 1.05 ppm. This confirms that the rate of exchange of the axial base is slow on the NMR time scale and indicates that the strap is somehow rejected away from the anisotropic current shift to allow the coordination of the nitrogen base. Single crystals suitable for X-ray diffraction were obtained by slow evaporation of a solution of **1Zn** in a mixture of methanol and pentane. In the solid state, the complex, as expected, is five coordinate (Figure 2) with two independent molecules in the cell unit (Table 1).[15]

Thus, only one of the two intramolecular pyridine cycles of the complex is coordinated to the zinc atom, by pulling it outside of the 24-atom mean plane of 0.478 Å with a resulting N5(pyr)−Zn bond length of 2.150 Å. The average length for the four N−Zn bonds is 2.042 Å, but the zinc atom is slightly shifted in the plane of the porphyrin toward the two meso

(10) Altomare, A.; Burla, M. C.; Camalli, M.; Cascarano, G.; Giacovazzo, C.; Guagliardi, A.; Moliterni, A. G. G.; Polidori, G.; Spagna, R. *J. Appl. Crystallogr.* **1999**, *32*, 115–119.

(11) Sheldrick, G. M. *SHELX97, Programs for Crystal Structure Analysis* (release 97−2); Institüt für Anorganische Chemie der Universiät: Göttingen, Germany, 1998.

(12) Farrugia, L. J. *J. Appl. Crystallogr.* **1999**, *32*, 837–838.

(13) Hijazi, I.; Roisnel, T.; Fourmigué, M.; Weiss, J.; Boitrel, B. *Inorg. Chem.* **2010**, *49*, 3098–3100.

(14) (a) Schauer, C. K.; Anderson, O. P.; Eaton, S. S.; Eaton, G. R. *Inorg. Chem.* **1985**, *24*, 4082–4086. (b) Scheidt, W. R.; Eigenbrot, C. W.; Ogiso, M.; Hatano, K. *Bull. Chem. Soc. Jpn.* **1987**, *60*, 3529–3533.

(15) Although two different molecules exist in the cell unit, only one will be discussed as the structural data and distortions discussed herein are quite similar. For detailed differences, see crystallographic CIF file of **1Zn** in Supporting Information.

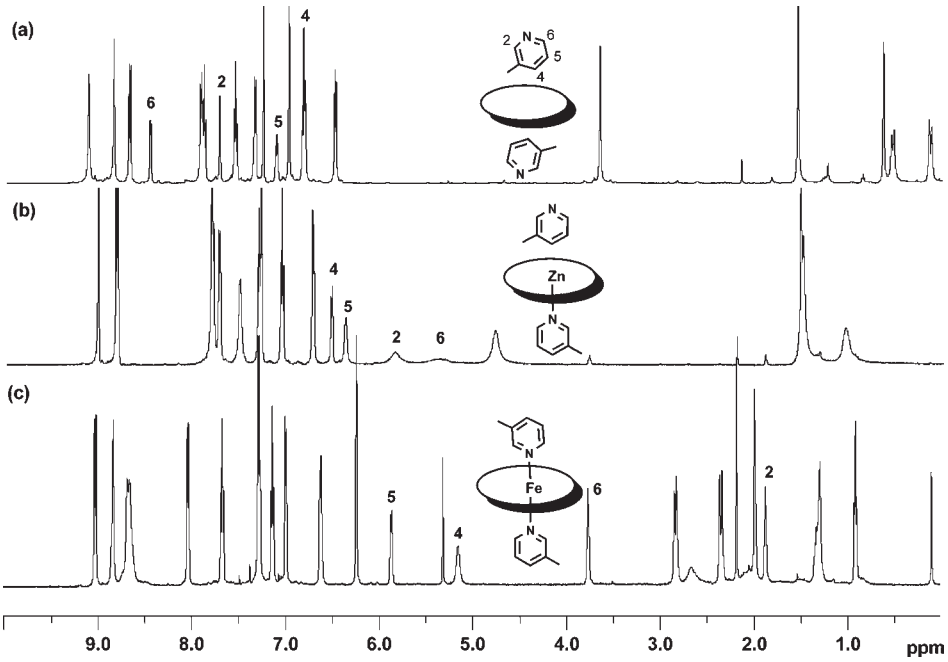

Figure 1. ^{1}H NMR spectra (500 MHz, $CDCl_3$, 298 K) of (a) free-base ligand **1**, (b) five-coordinate zinc(II) complex **1Zn**, and (c) six-coordinate iron(II) complex **1Fe(II)**.

Scheme 2. Synthesis of Zinc and Both Iron(II) and Iron(III) Complexes from the Free-Base **1**[a]

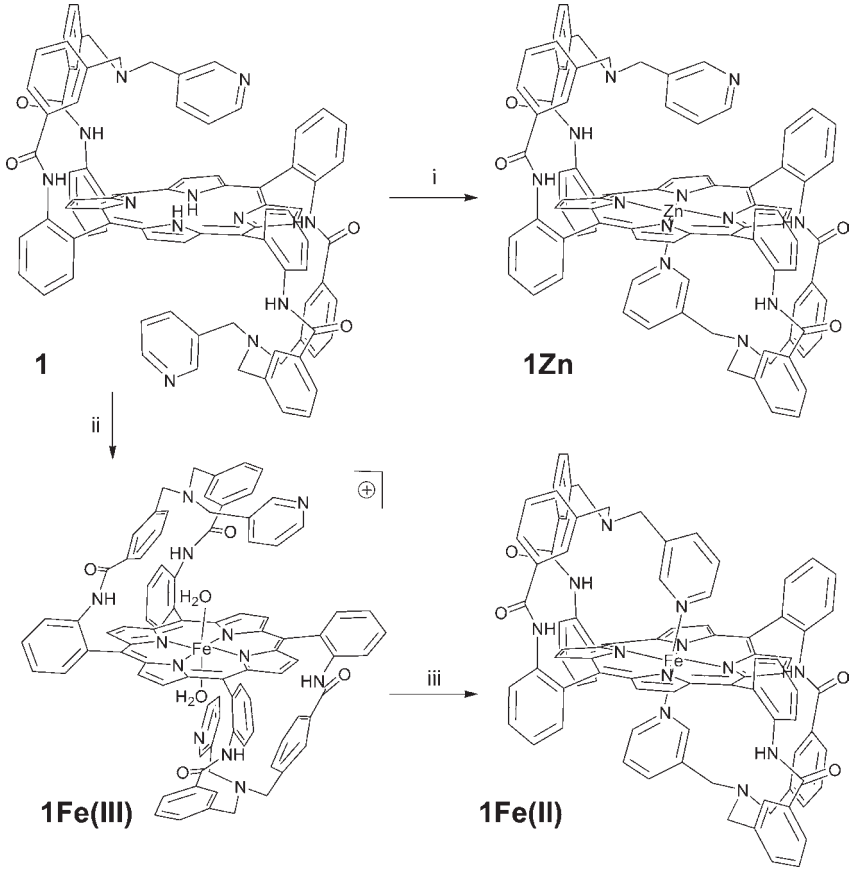

[a] (i) $AcONa/Zn(OAc)_2$, $CHCl_3$, MeOH, 60 °C, 92%; (ii) $FeBr_2$/ THF, 70 °C, overnight then air exposure; and (iii) aqueous $Na_2S_2O_4$, water, quantitative yield.

carbon atoms on which is tethered the coordinated pyridinyl strap, as indicated by the various N−Zn bond lengths (N4−Zn = 2.036, N3−Zn = 2.093, and N2−Zn = N1−Zn = 2.067 Å). However, these values compared well with

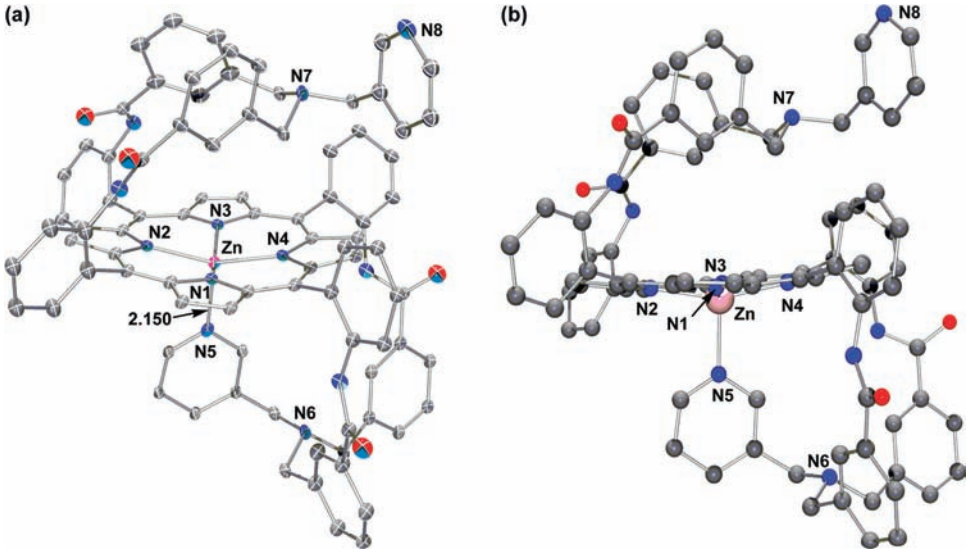

Figure 2. X-ray structure of complex **1Zn**. (a) Oak Ridge thermal ellipsoid plot (ORTEP, 30% thermal ellipsoids) perspective representation and (b) edge-on ball and stick view.

Table 1. Details of Data Collection, Structure Solution and Refinement for **1Zn**, **1Fe(II)**, and **1Fe(III)**

	1Zn	**1Fe(II)**	**1Fe(III)**
T, K	100(2)	100(2)	150(2)
formula	$2(C_{88}H_{64}N_{12}O_4Zn)$	$C_{88}H_{64}FeN_{12}O_4$, $4(CHCl_3)$	$C_{88}H_{64}Br_2FeN_{12}O_6$
formula weight	2837.76	1886.8	1601.18
crystal color	pink purple	red orange	red brown
crystal system	orthorhombic	monoclinic	orthorhombic
space group	$Pbc2_1$	$P2_1$	$Fdd2$
a, Å	19.704(4)	14.3242(6)	12.7796(5)
b, Å	23.194(4)	16.2707(9)	27.5987(9)
c, Å	35.517(7)	19.9354(10)	49.8342(17)
α, °	90	90	90
β, °	90	110.157(3)	90
γ, °	90	90	90
V, Å^3	16 232(5)	4361.7(4)	17 576.5(11)
radiation (λ, Å)	Mo Kα (0.71073)	Mo Kα (0.71073)	Mo Kα (0.71073)
Z	4	2	8
d_{calcd}, g·cm^{-3}	1.161	1.437	1.210
μ, mm^{-1}	0.359	0.600	1.137
$F(000)$	5904	1932	6560
no. of unique data	32 443	19 815	9996
no. of restraints	61	1	1
no. of params. refined	855	1091	494
GOF on $F2$	0.891	1.031	0.949
$R1^a$ [$I > 2\sigma(I)$]	0.1041	0.0669	0.0792
$R1^a$ (all data)	0.2359	0.1089	0.1422
$wR2^b$ (all data)	0.2555	0.1733	0.2249

$^aR1 = \sum||F_o| - |F_c||/\sum|F_o|$. $^bwR2 = \{\sum[w(F_o^2 - F_c^2)^2]/\sum[w(F_o^2)^2]\}^{1/2}$.

known similar five-coordinate porphyrinic complexes.[16] It is also worth noting that the strap delivering the nitrogen base around the coordination site is somehow too long, as seen in Figure 2b. Indeed, it is obvious that the relaxed position of the strap is bent at ca. 45° over the porphyrin core with the nitrogen atom N8 of the uncoordinated pyridine located at 4.6 Å away from the apical at the zinc atom. Furthermore, the observation of the coordinated strap shows that the latter has to stay in an orthogonal position relative to the porphyrinic plane to allow the pyridine nitrogen atom N5 to coordinate the zinc. Obviously, these steric strengths induce various distortions in the porphyrin as, in addition to the domed distortion expected for an out-of-plane square pyramidal polyhedron, both significant ruffled and saddled distortions are also observed (Figure 6). Indeed, the out-of-plane distortion of any porphyrin can be decomposed in a linear combination of six types of deformation that are known as saddled (sad), ruffled (ruf), domed (dom), waved(x) (wav(x)), waved(y) (wav(y)), and propeller (pro) according to the Normal-Coordinate Structural Decomposition (NSD) software of Shelnutt et al.[17] When the zinc complex **1Zn** is analyzed by

(16) (a) Bobrik, M. A.; Walker, F. A. *Inorg. Chem.* **1980**, *19*, 3383–3390. (b) Collman, J. P.; Schwenninger, R.; Rapta, M.; Bröring, M.; Fu, L. *Chem Commun* **1999**, 137–138. (c) Hamazawa, A.; Nishioka, T. Y.; Kinoshita, I.; Isobe, K.; Yano, S.; Wright, L. J.; Collins, T. J. *Chem. Lett.* **2003**, *32*, 20–21.

(17) (a) Jentzen, W.; Song, X. -Z.; Shelnutt, J. A. *J. Phys. Chem. B* **1997**, *101*, 1684–1699. (b) Sun, L.; Shelnutt, J. *The Normal-Coordinate Structural Decomposition Engine*; Scandia National Laboratories: Albuquerque, NM ; http://jasheln.unm.edu/jasheln/content/nsd/NSDengine/start.htm. Accessed 2010.

this method (Figure 6), equal and significant saddling and doming of the macrocycle are observed (−0.32 Å), and a subsequent ruffling (+0.25 Å) accompanies the saddling. These distortions are usually observed when an intramolecular coordinating group on one side of the porphyrin induces some steric hindrance to the macrocycle to reach the metal in the porphyrin.[18]

However, if in **1Zn** the saddled distortion is mostly due to some lack of flexibility of the ligand and the domed distortion can be attributed to the out-of-plane square pyramidal coordination of the zinc atom, in a complex in which the two pyridine are bound to the central metal, the domed distortion should disappear, whereas the saddling should remain predominant. In this connection, iron(II) (CN = 6, low-spin) has a similar ionic radius (0.61 Å) to that of zinc(II) (CN = 5) (0.68 Å),[19] and the iron(II) complex **1Fe(II)** should be six coordinate, octahedral, and diamagnetic with both pyridine coordinated to the metal center.

Thus, iron was inserted in porphyrin **1** according to the following procedure. In a drybox, porphyrin **1** was heated in THF with iron bromide overnight. The solvent was evaporated, and the residual solid was taken out of the drybox for convenient purification purposes by preparative layer chromatography, and then, once back in the drybox, reduced by sodium dithionite. As for the zinc complex, the coordination of the intramolecular pyridine bases was easily verified in solution by proton NMR spectroscopy (Figure 1, bottom trace), in comparison to both the free-base ligand in which none of the pyridines is coordinated and the zinc complex in which only one pyridine is coordinated. At a first glance, the NMR spectrum itself spanning from 10 to 0 ppm clearly indicates that the complex is diamagnetic and therefore six coordinate. It is also worth mentioning that this complex is air stable for several hours.

According to a more accurate analysis, the two protons in ortho position of the pyridine are strongly upfield shifted at 1.8 and 3.7 ppm for H_2 and H_6, respectively. On the other hand, the AB system relative to the benzylic methylene groups of the straps is downfield shifted from 0.18/0.58 ppm in the free base to 2.3/2.8 ppm in **1Fe(II)**, indicating as for **1Zn**, a quasi-orthogonal position of the strap relatively to the mean porphyrin plane. Fortunately, we were able to obtain single crystals suitable for X-ray diffraction by slow evaporation of a solution of **1Fe(II)** in a mixture of chloroform and methanol. The ORTEP view of this complex is represented in Figure 3.

This first crystal structure of a six-coordinate iron(II) complex with two intramolecular pyridine bases bound to the iron atom exhibits a highly distorted macrocycle which adopts a waved shape. The structure is not centro-symmetric, and the iron center is slightly out of the 24-atom mean plane (0.007 Å). Considering this complex, it is obvious that the straps do induce a severe distortion to the porphyrin core to allow the correct location of both axial bases on the metal center. As a result, the NSD analysis of **1Fe(II)** (Figure 6) shows that the ruffling is the predominant out-of-plane distortion, together with some residual saddling and waving-(x). The two pyridine cycles are not perpendicular to the

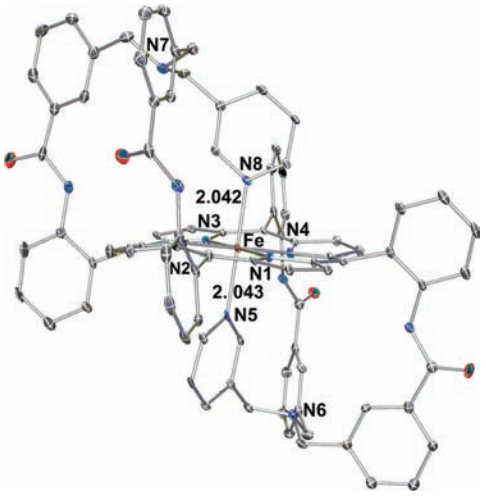

Figure 3. ORTEP (30% thermal ellipsoids) representation of complex **1Fe(II)**.

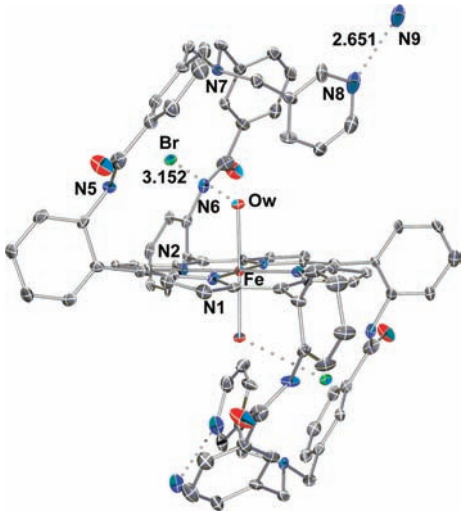

Figure 4. ORTEP (30% thermal ellipsoids) representation of complex **1Fe(III)**.

porphyrin mean plane but exhibit an angle of 75° and 82°, with a dihedral angle of 61° between the two pyridines. This orientation is likely to be dictated by steric restrictions imposed by the fact that the axial ligands are delivered to the iron center by a rigid strap. However, such an orientation has also been recently reported for bis(imidazole)iron(II) picket fence derivatives in which the two axial bases are not linked to the porphyrin.[20] The pyridine nitrogen-to-metal bond length is 2.042 Å, an expected value quite similar to that reported for $TPPFe(pyr)_2$[21] or other low-spin (porphyrinato)-iron(II) derivatives[22] and so are the four porphyrin nitrogen-to-metal bond lengths of 1.993, 2.000, 1.990, and 2.012 Å. The average Np−Fe−Np angle is ideal with a value of 90.00°. In other terms, although the carbon skeleton is significantly distorted, the polyhedron of coordination of iron in **1Fe(II)** is quite regular.

(18) (a) Boitrel, B.; Baveux-Chambenoit, V.; Richard, P. *Eur. J. Org. Chem.* **2001**, 4213–4221. (b) Boitrel, B.; Halime, Z.; Michaudet, L.; Lachkar, M.; Toupet, L. *Chem. Commun.* **2003**, 2670–2671. (c) Halime, Z.; Lachkar, M.; Furet, E.; Halet, J.-F.; Boitrel, B. *Inorg. Chem.* **2006**, *45*, 10661–10669.

(19) Shannon, R. D. *Acta Crystallogr.* **1976**, *A32*, 751–753.

(20) Li, J.; Nair, S. M.; Noll, B. C.; Schulz, C. E.; Scheidt, W. R. *Inorg. Chem.* **2008**, *47*, 3841–3850.

(21) TPP: dianion of meso-tetraphenylporphyrin. Li, N.; Coppens, P.; Landrum, J. *Inorg. Chem.* **1988**, *27*, 482–488.

(22) Scheidt, W. R.; Reed, C. A. *Chem. Rev.* **1981**, *81*, 543–555.

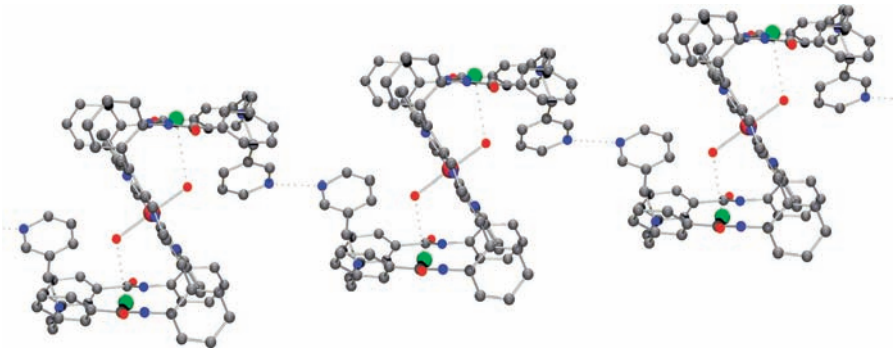

Figure 5. Ball and stick drawing of the solid-state structure of **1Fe(III)** emphasizing the spatial arrangement of several porphyrin units through the pyridinium−pyridine hydrogen bond wiring.

However, the situation is different with its oxidized counterpart, **1Fe(III)**. Indeed, as already mentioned, our synthetic procedure to isolate the ferrous complex, discussed above, went through the purification of the ferric complex, a process much easier to perform outside a glovebox. Before, to perform the reduction, we were also able to obtain single crystals of **1Fe(III)** by evaporation of a solution of the complex in a mixture of chloroform/methanol/pentane. Its X-ray structure determination reveals a centro-symmetric structure whose ORTEP representation appears in Figure 4. See also Figure 5 for the ball and stick structure of **1Fe(III)**.

It can be readily noted that, quite surprisingly, none of the pyridine ligands is bound to the iron center. Instead, the metal is six coordinate with two water molecules as the axial ligands. The Fe−Np distances are 2.100, 2.061, and 2.009 Å clearly indicating that the iron(III) ion is high-spin since these distances are substantially longer than those found for six-coordinated ferric porphyrins.[23] These longer distances reveal a radial expansion of the macrocycle as indicated by the in-plane displacements of the atoms of the porphyrin (Figure 7). Actually, although the in-plane distortions are much less used than their out-of-plane analogues (Figure 6), they can also be calculated by the NSD software mentioned above and are particularly useful to quantify and identify distortions as radial expansion (A1g), see Figure 7. In the case of **1Fe(III)**, it is obvious that the radial expansion is much more important (0.17 Å) than for **1Fe(II)** (0.045 Å), although the radius of iron(II) is larger than that of iron(III). This indicates that the d_{x2-y2} is occupied by an electron and therefore is consistent with an S = 5/2 spin state. The F−Ow (water) distance is 2.090 Å, an identical value than that reported for $[FeTPP(OH_2)_2]$[24] but slightly longer than that reported by Rath et al. for the same complex, but in which, the two water molecules are hydrogen bonded to the solvent THF and ClO_4.[25] The Np−Fe−Np angles are measured at 89.54° and 90.46°, and the two iron-to-oxygen bonds are not exactly perpendicular to the 24-atom mean plane as the angle Ow−Fe−Ow is 176.09°. This can be a direct result of the ruffling distortion (0.32 Å) of the macrocycle (Figure 6) without any contribution of either saddling or doming.

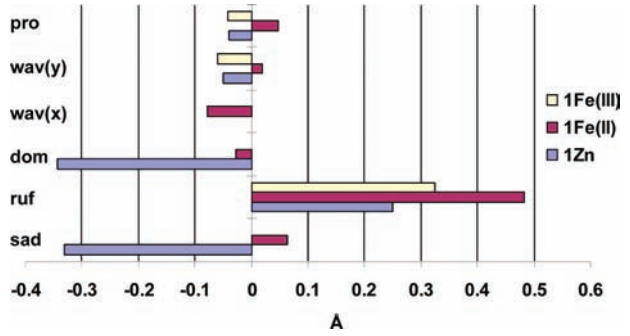

Figure 6. NSD of the out-of-plane displacements (Å) of the minimal basis for the X-ray crystal structures of **1Zn** (blue), **1Fe(II)** (purple), and **1Fe(III)** (pale yellow).

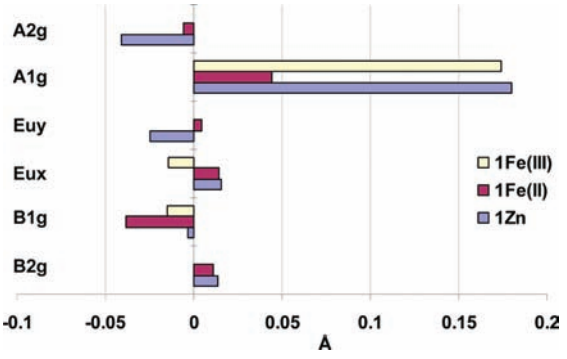

Figure 7. NSD of the in-plane displacement (Å) of the minimal basis for the X-ray crystal structures of **1Zn** (blue), **1Fe(II)** (purple), and **1Fe(III)** (pale yellow). (A1g corresponds to the radial expansion).

The oxidation state of iron in the two studied complexes **1Fe(III)** and **1Fe(II)** was investigated by voltammetry. Linear sweep voltammetry at a rotating disk electrode showed for **1Fe(III)** a reduction wave with a half-wave potential around 0.10 V_{SCE}, whereas the voltammogram of its reduced form **1Fe(II)** exhibited an oxidation wave in the same potential region (Figure 8).

Voltammetry experiments revealed that the complex **1Fe(II)** was air stable for several hours but was slowly oxidized to **1Fe(III)** after long-term air exposure, leading to an Fe(III):Fe(II) ratio of about 2:1 after two months (Figure 9).

The liquid helium EPR spectrum of the oxidized form of **1Fe(II)** dissolved in chloroform is represented in Figure 10. The signal is typical of high-spin Fe(III) with two effective g-values, $g_{\perp} = 5.92$ and $g_{//} = 2.00$.[25] The Fe(III):Fe(II) ratio was then probed by magnetization measurements on the

(23) Scheidt, W. R. In *The Porphyrin Handbook*; Kadish, K. M., Smith, K. M., Guilard, R., Eds.; Academic Press: San Diego, CA, 2000; Vol. *3*, p 49.
(24) (a) Kastner, M. E.; Scheidt, W. R.; Mashiko, T.; Reed, C. A. *J. Am. Chem. Soc.* **1978**, *100*, 666–667. (b) Scheidt, W. R.; Cohen, I. A.; Kastner, M. E. *Biochemistry* **1979**, *18*, 3546–3552.
(25) Patra, R.; Chaudhary, A.; Ghosh, S. K.; Rath, S. P. *Inorg. Chem.* **2008**, *47*, 8324–8335.

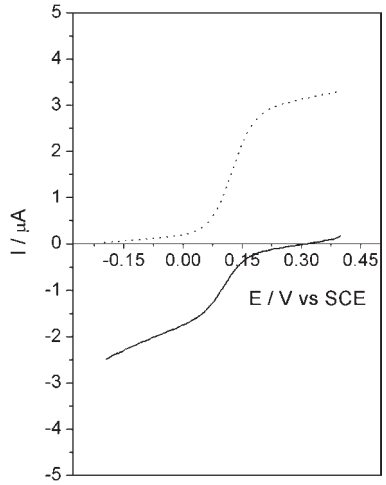

Figure 8. Current−voltage curves of the **1Fe(III)** complex (—) and its reduced form **1Fe(II)** (---) in acetonitrile + 0.1 M Bu_4NPF_6 at a vitreous carbon rotating disk electrode (400 rpm). Scan rate: 0.02 V s^{-1}.

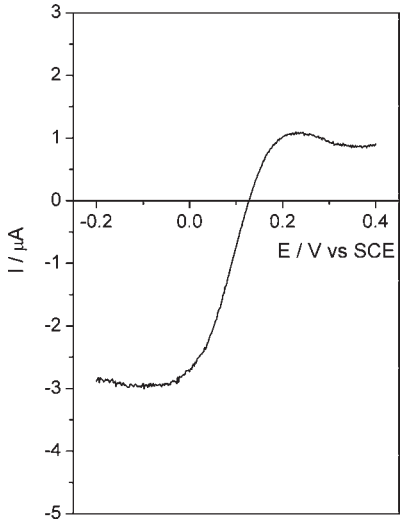

Figure 9. Current−voltage curves of the **1Fe(II)** complex after air exposure for two months, in acetonitrile + 0.1 M Bu_4NPF_6 at a vitreous carbon rotating disk electrode (500 rpm). Scan rate: 0.01 V s^{-1}.

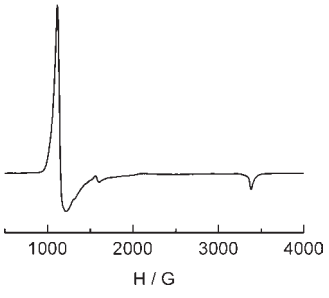

Figure 10. EPR spectrum at liquid helium temperature of **1Fe(III)** dissolved in chloroform.

same solid sample used for EPR and cyclic voltammetry. The temperature dependence of the product $\chi_M T$, χ_M being the magnetic molar susceptibility and T the temperature in Kelvin, is plotted in Figure 11. At room temperature $\chi_M T$ is equal to 2.81 cm^3 K mol^{-1} which is much lower than expected for high-spin (S = 5/2) Fe(III) species. On cooling, $\chi_M T$ remains almost constant down to 50 K then decreases on

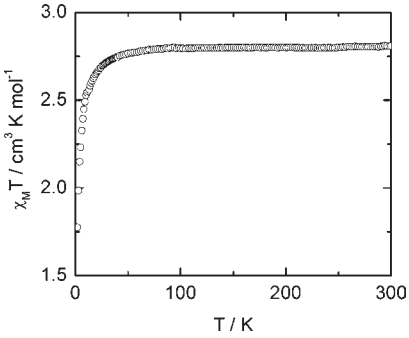

Figure 11. Temperature dependence of $\chi_M T$ of a powdered sample of **1Fe(III)**.

cooling further to reach 1.77 cm^3 K mol^{-1} at 2 K. This behavior is typical of isolated spins with zero-field splitting (ZFS).[26] Zeeman factor of high-spin Fe(III) is very close to 2.00 so the Curie constant of Fe(III) should be close to 4.375 cm^3 K mol^{-1}. SQUID susceptibility measurements revealed a signal corresponding to 64% (2.81 cm^3 K mol^{-1}) of the expected value. This result is in very good agreement with cyclic voltammetry (67% of Fe(III) and 33% of Fe(II)), considering that Fe(II) is in low-spin state (diamagnetic).

A particular detail in the structure of **1Fe(III)** is the weak hydrogen bond (3.152 Å) found between the axially iron-bound water molecules and a bromide atom (Fe−Ow−Br = 113.61°) bound by weak interactions inside the macrocycle formed by the straps. Indeed, the closest atom (N7) of the ring formed by the strap is located 3.280 Å away from the bromine atom, the two other nitrogen atoms N5 and N6 being at a distance of 3.973 and 3.628 Å, respectively. Actually, one bromine atom is the counteranion of the iron(III) ion inside the porphyrin, and the second bromide is the counteranion of an intramolecular pyridinium cation that was protonated by a HBr molecule, presumably during the metalation process. Although this proton was not observed in the X-ray structure, its presence is betrayed by the strong intermolecular hydrogen bond between N8(pyr) and N9(pyr), one of the two pyridine cycle acting as the hydrogen donor, leading the hydrogen-bond wire between porphyrin units displayed in Figure 5.

Conclusion

We have presented a series of three complexes obtained from the same ligand bearing two potential axial ligands delivered by a rigid, yet flexible strap. The structure of each complex was reported and their coordination sphere analyzed. The iron(III) complex represents a novel example to some scarce bis-aqua iron(III) complexes in which the metal lies in the plane of the porphyrin. The bromide counteranion of iron(III) is bound by electrostatic weak interactions as well as a hydrogen bond with an axially coordinated water molecule. Furthermore, none of the pyridinic bases from the ligand interact with the metal. A priori, this lack of coordination could be rationalized by a too high steric hindrance or rigidity of the strap. However, the X-ray structure of both the zinc and the iron(II) complexes show that either one- or two-pyridine coordination is possible with this ligand. Thus, the particular

(26) Kahn, O. *Molecular Magnetism*; VCH: New York, 1993.

structure of the iron(III) complex is mostly attributed to the synthetic procedure that allowed the protonation of one pyridine cycle during the metalation process. Additionally, the presence of the bromide counteranion in the reactional mixture during the purification process but also the peculiar shape and size of the macrocycle formed by the strap of the ligand that seems to fit well with the ionic radius of bromide are consistent with the observed structure.

Acknowledgment. The authors thank the CNRS for financial support as well as the MENRT for a grant for I.H. B.B. particularly acknowledges the CHEMBLAST program (Grant BLAN 0230) of the National Research Agency and Région Bretagne for his significant financial support.

Supporting Information Available: crystallographic CIF file of **1Zn**. This material is available free of charge via the Internet at http://pubs.acs.org.